

# Micromixing and Macromixing Effects in Unsteady Chemical Reaction System

P. C. Chang,<sup>†</sup> C. Y. Mou,<sup>†</sup> and D. J. Lee<sup>\*,‡</sup>

Department of Chemistry and Department of Chemical Engineering, National Taiwan University, Taipei, Taiwan, ROC

Received: February 3, 1999; In Final Form: April 28, 1999

This study presents a novel model that combines the tank-in-series model and the random replacement IEM (interaction by exchange with a mean environment) model for investigating the effects of both imperfect micromixing and macromixing. Two unstable chemical reaction model systems are simulated, the Oregonator model and the pH oscillator model. Dynamical behaviors include steady state, relaxation oscillation, small oscillation, and chemical chaos. Simulation results revealed significant effects of mixing; however, the ways the system dynamics had been altered depended on the chemical reaction systems.

## Introduction

Reactions of nonlinear chemical systems often involve initial contact of two miscible fluids upon mixing. The mixing efficiency could alter the system dynamics such as chemical selectivity and product distribution. Perfect mixing never exists for most reaction conditions, but in the past, studies of the dynamics of nonlinear chemical systems assumed mostly perfect mixing.<sup>1</sup> In real reaction systems, inhomogeneity due to imperfect mixing could affect system dynamics severely. The effect of mixing on oscillating chemical reactions has been a source of interest and even some controversy over the past decade, especially with respect to the appearance of chemical chaos. The problem is concerning the often assumed uniformity of a stirred reactor.<sup>2</sup>

In a reactor, the concentration segregation and its gradient could exist if the mechanical stirring or mass transfer by way of molecular diffusion is not fast enough. In nonlinear chemical reaction systems, the inhomogeneity further changes the behaviors of unsteady-state dynamics.<sup>3,4</sup> The effect of mixing is usually discussed in terms of micromixing and macromixing.<sup>3</sup> Macromixing is concerned with mixing on a macroscopic scale, usually the Kolmogoroff scale at about 50  $\mu\text{m}$ , caused by the average velocity field. On the other hand, micromixing is concerned with contact and mixing on a molecular scale. Macromixing is governed by mechanical stirring while micromixing is dominated by way of molecular diffusion. Macromixing can be treated essentially as an ordinary exchange between coupled reactors. Zonal models are widely employed for modeling the macromixing process.<sup>4–14</sup> One type of zonal model is the tank-in-series model, in which the reactor corresponds to many CSTRs connected to each other. A larger number of CSTRs corresponds to poorer macromixing.

The IEM (interaction by exchange with a mean environment) model is one of the most commonly applied micromixing models, partially owing to its simplicity.<sup>15–20</sup> In an IEM-type model, each fluid parcel entering the reactor is assumed to exchange mass with the mean fluid field with a characteristic time,  $t_m$ . The concentration of fluid field is calculated directly from averaging over all fluid parcels in the reactor. One of its

major disadvantages is the difficulty in dealing with stiff chemical kinetics.

Chang et al.<sup>21</sup> refined the original IEM model<sup>2</sup> by improving its capability of taking care of stiff chemical kinetics, such as the Oregonator model<sup>22</sup> (discussed later). The so-called “random replacement IEM model” adopted a molecular dynamics-like scheme that could be applied in investigating the effects of imperfect micromixing.<sup>21</sup>

The perfect solution for some applications requires the consideration of both macromixing and micromixing, but researchers rarely consider a model treating the combined effects of both levels of mixing. This study proposes such a model, combining the tank-in-series model and the random replacement IEM model. The study simulates two dynamically unstable reaction model systems: the Oregonator model<sup>22</sup> and the pH oscillator.<sup>23</sup> The possible stirring effects of the latter model had never been explored. We investigated herein the effects of imperfect micromixing and macromixing on their dynamical behaviors.

## The Mixing Models

The random replacement IEM model<sup>21</sup> calculates the mass balance for the fluid parcel of age  $\alpha$  in the premixing mode as follows:

$$\frac{dC_i(\alpha)}{dt} = \frac{1}{t_m}[\langle C \rangle - C_i(\alpha)] + R(C_i(\alpha)) \quad (1)$$

where  $C_i$  denotes the concentration vector in the  $i$ th fluid parcel,  $t_m$  is the mixing time, and  $R$ , is the chemical reaction term. There are a total of  $N$  parcels in the tank. We choose  $N$  in an increasing order until the simulation results appear unchanging. In this paper, the  $N$  value we found to be proper is 500 for the two models we consider.

In a perfectly macromixed CSTR, the residence time of the fluid parcels would follow an exponential distribution of  $(1/\tau)\exp(-\alpha/\tau)$  where  $\tau$  is the residence time. Each parcel in the tank has an equal probability of leaving the perfectly macromixed reactor at time  $t$ . Consequently, repeatedly and randomly replacing an old parcel from the reactor, regardless of its age, with a new parcel of age 0, at a time interval of  $\Delta\alpha(=\tau/N)$ , leads to a stationary, exponential-type residence time distribu-

<sup>†</sup> Department of Chemistry.

<sup>‡</sup> Department of Chemical Engineering.

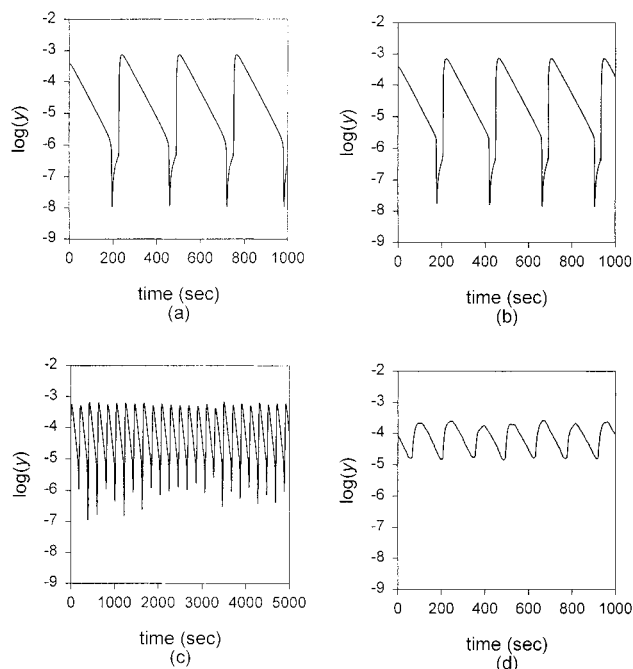


**Figure 1.** Time evolutions of mean field concentration of  $y$  in a perfectly macromixed reactor with the Oregonator model of various micromixing times. (a)  $t_m = 0.1$ , relaxation oscillation occurs if the micromixing is not too inefficient; (b)  $t_m = 10$ , as  $t_m$  increases the period of oscillation decreases with its amplitude decreasing; (c)  $t_m = 46$ , in the intermediate region there exist chaotic oscillations; (d)  $t_m = 150$ , at very poor micromixing the oscillations become random in both frequency and amplitude. The large number of coupled, stiff, ordinary differential equations were solved using stiff Gear integrator.<sup>24</sup>

tion. Such a stationary distribution of age enables working on the absolute time scale, taking the average concentration over the whole reactor as follows:

$$\langle C \rangle = \frac{1}{N} \sum_i C_i(t) \quad (2)$$

That is, the mean field concentration  $\langle C \rangle$  is evaluated taking into account all fluid parcels present in the reactor at time  $t$ , regardless of their age  $\alpha$ .

In the tank-in-series model, the concentration segregation can be viewed as many CSTRs connected to each other. The mass balance for the concentration vector in the  $i$ th fluid parcel in the  $L$ th CSTR,  $C_i^L$ , is in the form of eq 1. The corresponding mean concentration,  $\langle C^L \rangle$ , is averaged over the  $L$ th CSTR. The age distribution of the parcels is given as follows:

$$E(\alpha) = \left(\frac{M}{\tau}\right)^M \times \frac{\alpha^{M-1}}{(M-1)!} e^{-\left(\frac{M}{\tau}\right)\alpha} \quad (3)$$

where  $\alpha$  is the lifetime of fluid parcels and  $M$  is the total number of CSTRs.

The proposed combined model comprises  $M$  CSTRs connected in a series; in each CSTR there are  $N/M$  fluid parcels. At a flow rate of  $1/\tau$ , during each period of  $\Delta\alpha (= \tau/N)$  a fresh fluid parcel was fed into tank 1 and an old parcel was randomly selected and transferred from tank 1 to tank 2. Meanwhile, a randomly selected parcel from tank 2 was moved to tank 3. This transfer process continued in all tanks. The outflow of the system was the randomly selected parcel removed from tank  $M$ . This model leads to the stationary residence time distribution of eq 3.

Two parameters in the combined model,  $t_m$  and  $M$ , can be adjusted. As the value of  $M$  rises, macromixing becomes poorer, and as the value of  $t_m$  falls, micromixing becomes better. With intermediate values of  $M$  and  $t_m$ , the combined effects of both imperfect macromixing and imperfect micromixing can thus be examined.

## Simulation Results

**Oregonator Model.** The Oregonator model, originally proposed by Field and Noyes,<sup>22</sup> is a skeletal model for the Belousov–Zhabotinsky (BZ) reaction as follows:



where  $A = [\text{BrO}_3^-]$ ,  $P = [\text{HOBr}]$ ,  $x = [\text{HBrO}_2]$ ,  $y = [\text{Br}^-]$ , and  $z = 2[\text{Ce}^{4+}]$ . The concentration of  $A$  is taken as constant,  $k_1$  to  $k_5$  are rate constants, and  $f$  is a stoichiometric parameter.<sup>25</sup> The corresponding kinetic equations (the Oregonator model) can be stated as follows:

$$\frac{dx}{dt} = k_1Ay - k_2xy + k_3Ax - 2k_4x^2 \quad (5-1)$$

$$\frac{dy}{dt} = -k_1Ay - k_2xy + fk_5z \quad (5-2)$$

$$\frac{dz}{dt} = k_3Ax - k_5z \quad (5-3)$$

The kinetic parameters include  $k_1 = 1.3 \text{ dm}^3 \text{ mol}^{-1} \text{ s}^{-1}$ ,  $k_2 = 2.4 \times 10^6 \text{ dm}^3 \text{ mol}^{-1} \text{ s}^{-1}$ ,  $k_3 = 34 \text{ dm}^3 \text{ mol}^{-1} \text{ s}^{-1}$ ,  $k_4 = 3000 \text{ dm}^3 \text{ mol}^{-1} \text{ s}^{-1}$ ,  $k_5 = 0.02 \text{ s}^{-1}$ ,  $f = 1$ , and  $A = 0.06 \text{ dm}^{-3} \text{ mol}$ . The flow rate is set at  $0.01 \text{ s}^{-1}$  ( $\tau = 100 \text{ s}$ ) with the inlet concentration  $(x_0, y_0, z_0) = (0, 0, 10^{-6} \text{ dm}^{-3} \text{ mol})$ . Under these circumstances, the Oregonator model exhibits a relaxation oscillation behavior of period 261 under perfect macromixing and micromixing conditions.

Figure 1 depicts the time evolutions of mean field concentrations of  $y$  in a perfectly macromixed reactor ( $M = 1$ ). Relaxation oscillation occurs if the micromixing is not too inefficient (Figure 1a). As  $t_m$  increases, the period of oscillation decreases with its amplitude decreasing, indicating shrinkage of the limit cycle attractor under imperfectly micromixed condition (Figure 1b). Such a result correlates well with previous work<sup>21</sup> and is parallel to the findings for an imperfectly macromixed (but perfectly micromixed) reactor.<sup>5</sup> At very poor micromixing the oscillations become random in both frequency and amplitude (Figure 1d). The phase portrait for the trajectory in Figure 1d appears to be a fuzzy ring without structure. In the intermediate region there exist chaotic oscillations (Figure 1c). The phase portrait becomes a strange attractor.

Figure 2 depicts the time evolutions of tank 1 in a somewhat imperfectly macromixed reactor ( $M = 2$ ). Oscillations occur only within a range of  $t_m$ . Under perfectly micromixed conditions ( $t_m = 0.1$ ), tank 1 is in the thermal-branch steady state (Figure 2a), while tank 2 is in the flow-branch steady state.

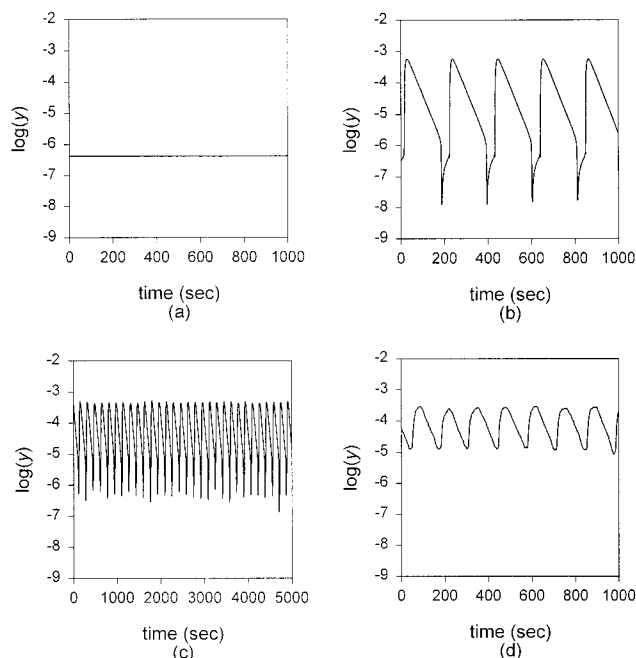


**Figure 2.** Time evolutions of tank 1 in an imperfectly macromixed reactor ( $M = 2$ ) with the Oregonator model of various micromixing times. (a)  $t_m = 0.1$ , under perfectly micromixed conditions tank 1 locates in thermal-branch steady state; (b)  $t_m = 5$ , the normal relaxation oscillations suddenly appear; (c)  $t_m = 46$ , the complex oscillations result with  $t_m$  increasing further as in the  $M = 1$  case; (d)  $t_m = 150$ , after the chaotic oscillation regime follows a low-amplitude oscillation regime.

Such a result is expected inasmuch as when the whole tank is divided into two CSTRs of equal volumes, the effective flow-through residence time has been halved. At  $t_m$  slightly exceeding 1.0, normal relaxation oscillations suddenly appear (Figure 2b), corresponding to a subcritical Hopf bifurcation. The oscillation sustains as  $t_m$  increases further, but with the limit cycle attractor shrinking as in the  $M = 1$  case. Around  $t_m = 45$  complex oscillations result. Figure 2c illustrates typical time evolution patterns.

After the chaotic oscillation regime follows a low-amplitude oscillation regime (Figure 2d). As  $t_m$  increases still further, the amplitude decreases continuously. Finally the oscillation decays to the flow-branch steady state, corresponding to a supercritical Hopf bifurcation.

Summarizing the observations as presented in Figure 2, we plot the phase diagram of dynamical behaviors in Figure 3 depicting the corresponding bifurcation. We show a large range of micromixing as the  $x$ -axis is  $\log(t_m)$ . From left to right, on increasing  $t_m$ , the dynamics change from steady-state I through a sudden subcritical Hopf bifurcation to a relaxation oscillation such as in Figure 2b. On the right-hand boundary, in a narrow range of  $t_m$ , the time evolutions cascade from simple oscillation (Figure 2b) to complex oscillation and then to chaos Figure 2c. In the narrow chaos range, the system exhibits chaotic oscillation in which the period appears constant over time but the amplitude is not regular (Figure 2c). After the chaos range, the system is the random oscillatory range with small amplitude (osc. II) as shown in Figure 2d. Finally through a supercritical transition, the system is in another steady state (s.s. II).

A similar bifurcation sequence is noted for cases with larger  $M$ . Figure 4 depicts the bifurcation diagram with  $M = 1, 2$ , and 5. As Figure 4 reveals, at poorer micromixing and/or macromixing, both the thermal-branch and the flow-branch steady states become more stable than the oscillatory state. With poor micromixing and macromixing, the oscillatory state of the

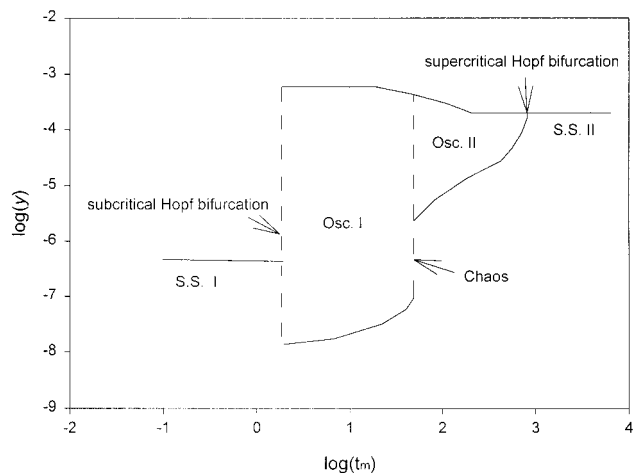
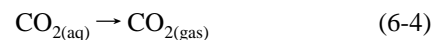
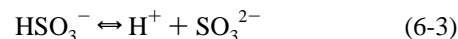
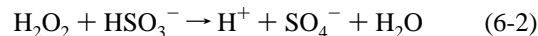
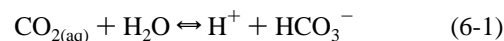


**Figure 3.** Bifurcation diagram of tank 1 in an imperfectly macromixed reactor ( $M = 2$ ) with the Oregonator model at various micromixing times.

Oregonator model tends to diminish. On the other hand, a complex oscillation regime persists regardless of the degree of macromixing. We note herein that when Oregonator model gives a steady state, periodic or aperiodic oscillations could be induced by imperfect mixing.

**pH Oscillator Model.** Rabai et al.<sup>23</sup> combined the acidic dissociation equilibrium of  $\text{CO}_2(\text{aq})$  (eq 6-1) with a slow removal of  $\text{CO}_2$  from the solution with an oscillatory  $\text{H}_2\text{O}_2$ – $\text{HSO}_3^-$  system and found chaotic change of pH in a CSTR. They proposed a pH oscillator as in the following:



The corresponding rate expressions are  $R_1 = k_1[\text{CO}_{2(\text{aq})}]$ ;  $R_{-1} = k_{-1}[\text{H}^+][\text{HCO}_3^-]$ ;  $R_2 = (k_1 + k_2'[\text{H}^+]) [\text{HSO}_3^-][\text{H}_2\text{O}_2]$ ;  $R_3 = k_3[\text{HSO}_3^-]$ ;  $R_{-3} = k_{-3}[\text{H}^+][\text{SO}_3^{2-}]$ ;  $R_4 = k_4[\text{CO}_{2(\text{aq})}]$ ;  $R_5 = k_5[\text{H}^+]$ . The rate constants include:  $k_1 = 0.011 \text{ s}^{-1}$ ;  $k_{-1} = 2.5 \times 10^4 \text{ dm}^3 \text{ mol}^{-1} \text{ s}^{-1}$ ;  $k_2 = 1.54 \text{ dm}^3 \text{ mol}^{-1} \text{ s}^{-1}$ ;  $k_2' = 6.5 \times 10^6 \text{ dm}^6 \text{ mol}^{-2} \text{ s}^{-1}$ ;  $k_3 = 1.0 \times 10^3 \text{ s}^{-1}$ ;  $k_{-3} = 1.0 \times 10^{10} \text{ dm}^3 \text{ mol}^{-1} \text{ s}^{-1}$ ;  $k_4 = 0.001 \text{ s}^{-1}$ ; and  $k_5 = 0.03 \text{ s}^{-1}$ . In addition, the feed flow rate is  $0.0006 \text{ s}^{-1}$  ( $\tau = 1667 \text{ s}$ ).

Figure 5 depicts the time evolutions of mean field concentration of  $y$  ( $\text{H}^+$ ) in a perfectly macromixed reactor ( $M = 1$ ). At a small  $t_m$  (less than 0.2), the system exhibits a complex oscillatory state with two periods, a fast oscillation embedded in big single period (Figure 5a), which correlates well with the experimental observation.<sup>23</sup> The fast oscillation may not be perfectly regular, but the large oscillation appears to be quite periodic. With an increase in  $t_m$ , prolonged periodic and more complex oscillation patterns appear (Figure 5b). Some of the large peaks miss its appearance and are replaced by small fast oscillations. So the evolution becomes complex and irregular. The oscillation period increases accordingly while the oscillation becomes more and more irregular. Such a result is opposite to that for the Oregonator model. At a poor micromixing ( $t_m > 1.0$ ) limit, the oscillation again becomes complex periodic with a longer period for the large oscillation (Figure 5c). The

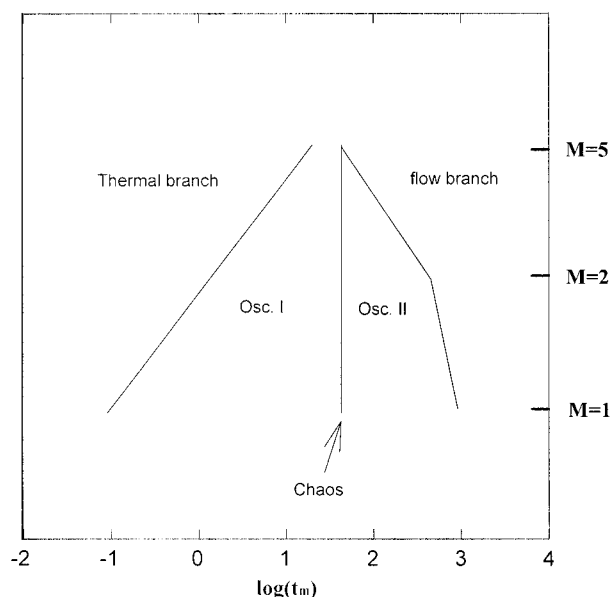


**Figure 4.** Bifurcation diagram with  $M = 1, 2,$  and  $5$  with the Oregonator model. s.s. I: thermal-branch steady state; Osc. I: relaxation oscillations; Osc. II: smaller amplitude oscillations; s.s. II: flow-branch steady state. At poorer macromixing both the thermal-branch and flow-branch steady state become more stable than the oscillatory state, but the complex oscillation regime persists regardless of the degree of macromixing.

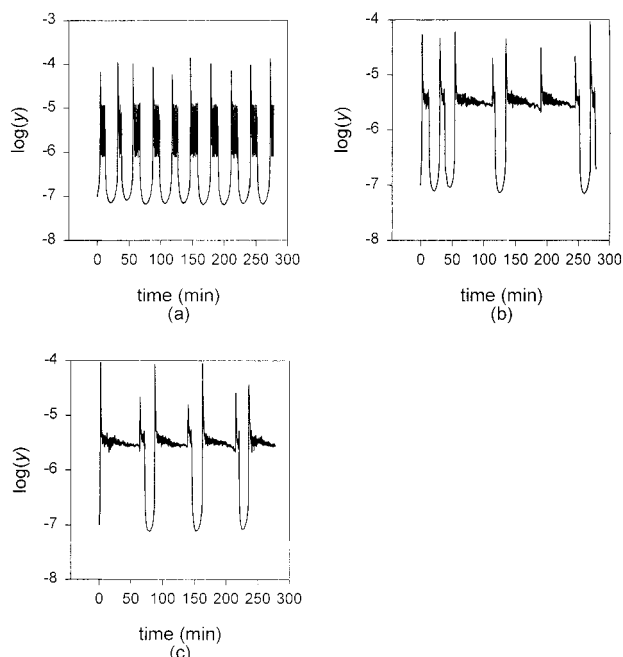


**Figure 5.** Time evolutions of mean field concentration of  $H^+$  in a perfectly macromixed reactor containing a pH oscillator. (a)  $t_m = 0.1$ , the system exhibits a complex oscillatory state with two periods under smaller  $t_m$ ; (b)  $t_m = 0.8$ , mixed oscillation mode composed of the two patterns as revealed in (a) and (c); (c)  $t_m = 1.0$ , at a poor micromixing ( $t_m > 1.0$ ), complex oscillation patterns with longer large period appear.

frequency of oscillations markedly increases. Between there is mixed oscillation mode composed of the two patterns revealed in Figure 5b. The mixed oscillation is stochastic in nature. At a still poorer micromixing the pattern changes into random oscillations with smaller amplitude. Finally the system transits to the flow-branch steady state via a supercritical Hopf bifurcation.

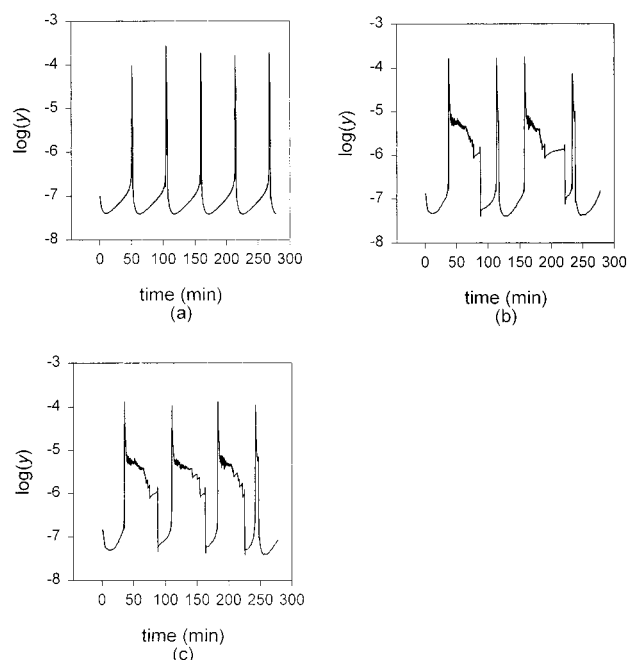


**Figure 6.** Time evolutions of tank 1 in an imperfectly macromixed reactor ( $M = 2$ ) with the pH oscillator model. (a)  $t_m = 0.1$ , tank 1 exhibits a simple relaxation oscillation at small  $t_m$ . As  $t_m$  increases similar evolutions as case ( $M = 1$ ) but with a more complex oscillation of mixed mode appear; (b)  $t_m = 0.8$ , and (c)  $t_m = 1.0$ .

Figure 6 depicts the time evolutions of tank 1 in an imperfectly macromixed reactor ( $M = 2$ ). Relaxation oscillations appear as the dominating state at the perfect mixing  $t_m \rightarrow 0$  limit. As  $t_m$  increases, a similar bifurcation as noted in the  $M = 1$  case is noted. However, the corresponding micromixing time where the system changes into thermal-branch steady state becomes higher, indicating a more stable oscillatory state. This result is in *opposition* to the Oregonator model. We thereby conclude that micromixing does have a significant effect on the pH oscillator model proposed by Rabai et al.<sup>23</sup> Macromixing, on the other hand, played a less significant role.

**Role of Macromixing and Micromixing.** According to the preceding discussions, macromixing and micromixing can markedly affect chemical dynamics. However, the two levels of mixing have distinct influences. Take the Oregonator model as an example. Poor micromixing favors a flow-branch steady state; the next preferred state is the oscillatory state, and the least favorable state is the thermal-branch steady state. The observation of enhancing the flow-branch steady state in a poorer micromixing environment correlates with previous findings for the Gray–Scott model.<sup>21</sup> However, for the first time, this study identifies the bifurcation sequence from thermal-branch steady state  $\rightarrow$  oscillatory state  $\rightarrow$  flow-branch steady state as micromixing gets worse (even at the perfect macromixing limit).

On the other hand, under perfect micromixing conditions, poor macromixing tends to destabilize the oscillatory state in the Oregonator model.<sup>6</sup> However, as the micromixing time becomes larger, the more favorable state becomes the flow-branch steady state. Of particular interest, is the case with an intermediate micromixing time, reflecting a normal mixing practice: the oscillatory state is sustained regardless of the macromixing efficiency.

These observations reveal that although macromixing and micromixing both affect chemical dynamics, there are certain distinct differences regarding their effects. A practical mixing apparatus usually provides an intermediately micromixed and intermediately macromixed environment. The combined effects

may lead to a complicated oscillation pattern, which may not occur when either micromixing or macromixing is perfect.

### Conclusions

This study presents a novel model that combines the tank-in-series model and the random replacement IEM model for investigating the situation with both imperfect micromixing and imperfect macromixing. Two unstable chemical kinetic systems were simulated: the Oregonator model and the pH oscillator; this is the first report on the effect of mixing on the pH oscillator model. Both macromixing and micromixing markedly affect the Oregonator model dynamics. When the Oregonator model is in a steady state, poor mixing can induce periodic and aperiodic oscillation. In addition, both thermal-branch and flow-branch steady states become more stable than the oscillatory state: under imperfect mixing, the period and amplitude of oscillation decrease accordingly. For the pH oscillator, on the other hand, poor micromixing leads to prolonged oscillation pattern: the frequency of oscillation increases rather than decreases as mixing time increases. Macromixing has a less significant effect on the pH oscillator model. Thus, the effects of stirring depend on the chemical reaction systems employed.

### Notations

|                       |   |
|-----------------------|---|
| $A$                   | $[\text{BrO}_3^-]$ , $\text{dm}^{-3}$ mol                             |
| $C_i$                 | concentration vector in the $i$ th fluid parcel, $\text{dm}^{-3}$ mol |
| $\langle C_i \rangle$ | average concentration vector in fluid parcel, $\text{dm}^{-3}$ mol    |
| $f$                   | stoichiometric parameter  |
| $k_i$                 | rate constants  |
| $M$                   | number of CSTRs   |
| $N$                   | number of fluid parcels   |
| $P$                   | $[\text{HOBr}]$ , $\text{dm}^{-3}$ mol                                |
| $R_i$                 | rate expression, $\text{dm}^{-3}$ mol $\text{s}^{-1}$                 |
| $t$                   | time  |

|                |  |
|----------------|--|
| $t_m$          | mixing time                                |
| $x$            | $[\text{HBrO}_2]$ , $\text{dm}^{-3}$ mol   |
| $y$            | $[\text{Br}^-]$ , $\text{dm}^{-3}$ mol     |
| $z$            | $2[\text{Ce}^{4+}]$ , $\text{dm}^{-3}$ mol |
| $\alpha$       | lifetime of fluid parcels                  |
| $\Delta\alpha$ | $\Delta\alpha = \tau/N$                    |
| $\tau$         | residence time                             |
| CSTR           | continue stirred tank reactor              |

### References and Notes

- (1) Scott, S. K. *Oscillations, Waves, and Chaos in Chemical Kinetics*; Oxford University Press: Oxford, U.K., 1994.
- (2) Epstein, I. R. *Nature* **1990**, *364*, 16.
- (3) Villermaux, J. *Rev. Chem. Eng.* **1991**, *7*, 51.
- (4) Dutt, A. K.; Menzinger, M. *J. Phys. Chem.* **1992**, *96*, 8447.
- (5) Bar-Eli, K.; Noyes, R. M. *J. Chem. Phys.* **1986**, *85*, 3251.
- (6) Hsu, T. J.; Mou, C. Y.; Lee, D. J. *J. Chem. Eng. Sci.* **1994**, *49*, 5291.
- (7) Hsu, T. J.; Lee, D. J. *J. Chem. Phys.* **1995**, *102*, 8274.
- (8) Hsu, T. J.; Mou, C. Y.; Lee, D. J. *J. Chem. Eng. Sci.* **1996**, *51*, 2589.
- (9) Ganapathisubramanian, N. *J. Chem. Phys.* **1991**, *95*, 3005.
- (10) (a) Gyorgyi, L.; Field, R. J. *J. Chem. Phys.* **1989**, *91*, 6131. (b) Gyorgyi, L.; Field, R. J. *J. Phys. Chem.* **1989**, *93*, 2865.
- (11) Hauser, M. J. B.; Lebender, D.; Schneider, F. W. *J. Phys. Chem.* **1992**, *96*, 9332.
- (12) Kumpinsky, E.; Epstein, I. R. *J. Chem. Phys.* **1985**, *82*, 53–57.
- (13) Liu, C. I.; Wen, H. J.; Lee, D. J. *J. Phys. Chem.* **1997**, *101*, 170.
- (14) Liu, C. I.; Wen, H. J.; Lee, D. J. *J. Chem. Phys. Lett.* **1997**, *271*, 167.
- (15) Fox, R. O. *Chem. Eng. Sci.* **1989**, *44*, 2831.
- (16) Fox, R. O. *Chem. Eng. Sci.* **1991**, *46*, 1829.
- (17) Fox, R. O.; Cutis, W. D.; Halasi, K. *Chem. Eng. Sci.* **1990**, *45*, 3571.
- (18) Fox, R. O.; Villermaux, J. *Chem. Eng. Sci.* **1990**, *45*, 373.
- (19) Fox, R. O.; Villermaux, J. *Chem. Eng. Sci.* **1990**, *45*, 2857.
- (20) Fox, R. O.; Erjaee, G.; Zou, Q. *Chem. Eng. Sci.* **1994**, *49*, 3465.
- (21) Lee, D. J.; Chang, P. C.; Mou, C. Y. *J. Phys. Chem.*, **1997**, *101*, 1854.
- (22) Field, R. J.; Noyes, R. M. *J. Chem. Phys.* **1974**, *60*, 1877.
- (23) Rabai, G.; Kaminaga, A.; Hanazaki, I. *Chem. Commun.* **1996**, 2181.
- (24) Kahaner, D.; Moler, C.; Nash, S. *Numerical Methods and Software*; Prentice Hall: Englewood Cliffs, N. J., 1989.
- (25) DeKepper, P.; Boissonade, J. *J. Chem. Phys.* **1981**, *75*, 189.